

A human scalable platform for high-throughput screening of drug candidates targeting pathological aggregation of TAU, α Synuclein and TDP-43



Jessica Koepke, Carola van Berkel, Leo Smit, Benoit Samson-Couterie, Shushant Jain

Ncardia Services BV Leiden, The Netherlands, support@ncardia.com, www.ncardia.com

Background

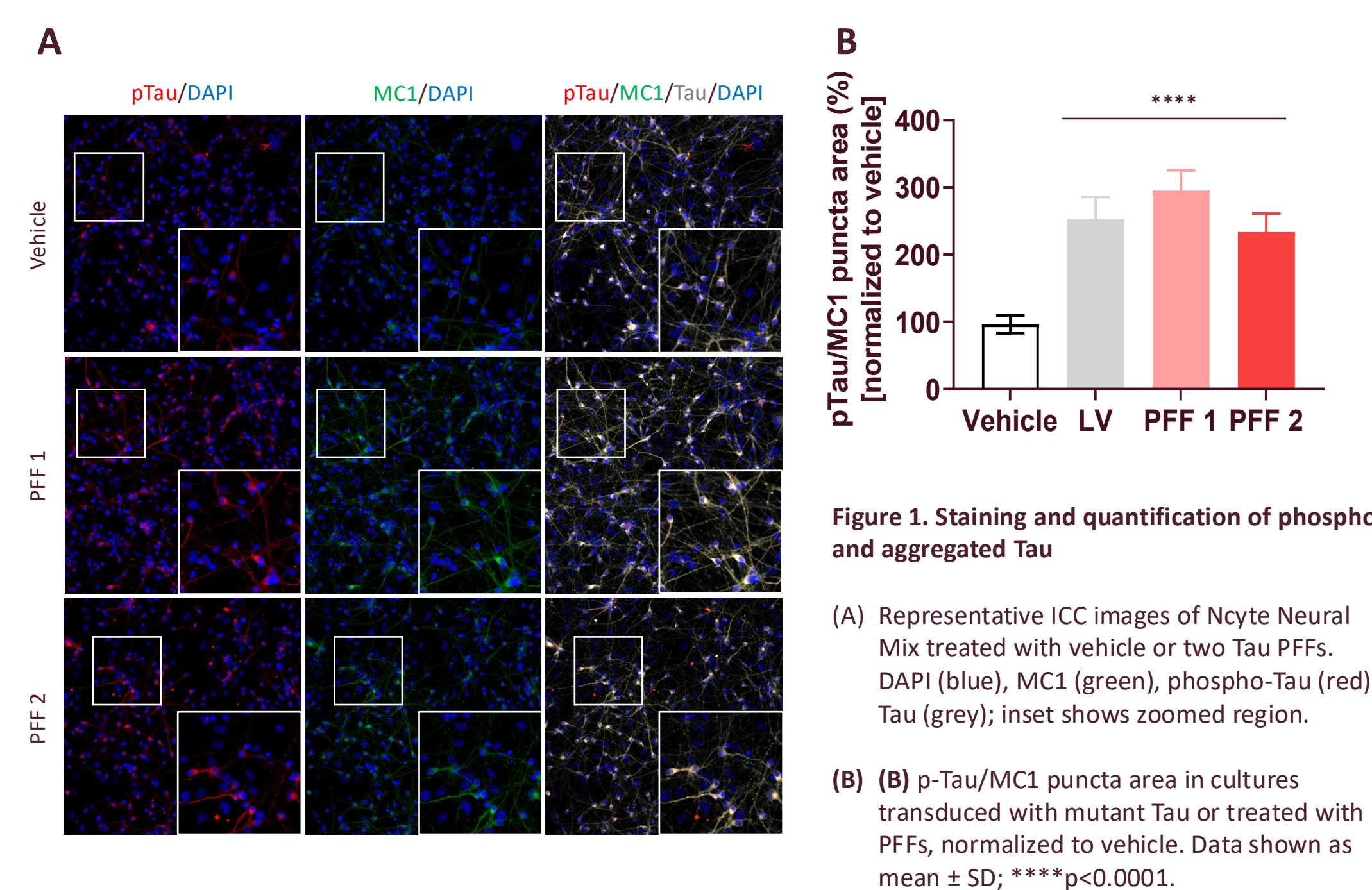
Neurodegenerative disorders are marked by the accumulation of misfolded proteins, a pathological feature. This aggregation is so critical to the understanding of these diseases that they are now categorized under the umbrella of proteinopathies. These categories are based on the type of protein that is most commonly found aggregated in each disorder.

Although protein misfolding, accumulation and aggregation is a major cause of neurodegeneration; there remains a major unmet need of physiologically-relevant models to both study the mechanism of propagation and aggregation, and to screen potential therapeutics.

At Ncardia, we have developed scalable models for tauopathies, synucleinopathies and TDP43 proteinopathies using human iPSC-derived stem cell technology (hiPSC). All these models have been miniaturized to 384-well format to make them suitable for high-throughput compound screening.

Tauopathies

For tauopathies using high content imaging (HCI) Ncardia demonstrated quantifiable presence of phosphorylated and neurofibrillary tangles of TAU in Ncyte[®] Neural Mix (co-culture of hiPSC-derived neurons and astrocytes) cultures compared to untreated control cultures.



Synucleinopathies

In our synucleinopathy models, Ncardia demonstrated that treatment with α -synuclein preformed fibril (PFF) on three different cultures, (1) Ncyte cortical neurons, (2) Ncyte Neural Mix (data not shown) and (3) dopaminergic neurons (data not shown) displayed statistically significant increases in pS129 by HCI as compared to untreated control cultures.

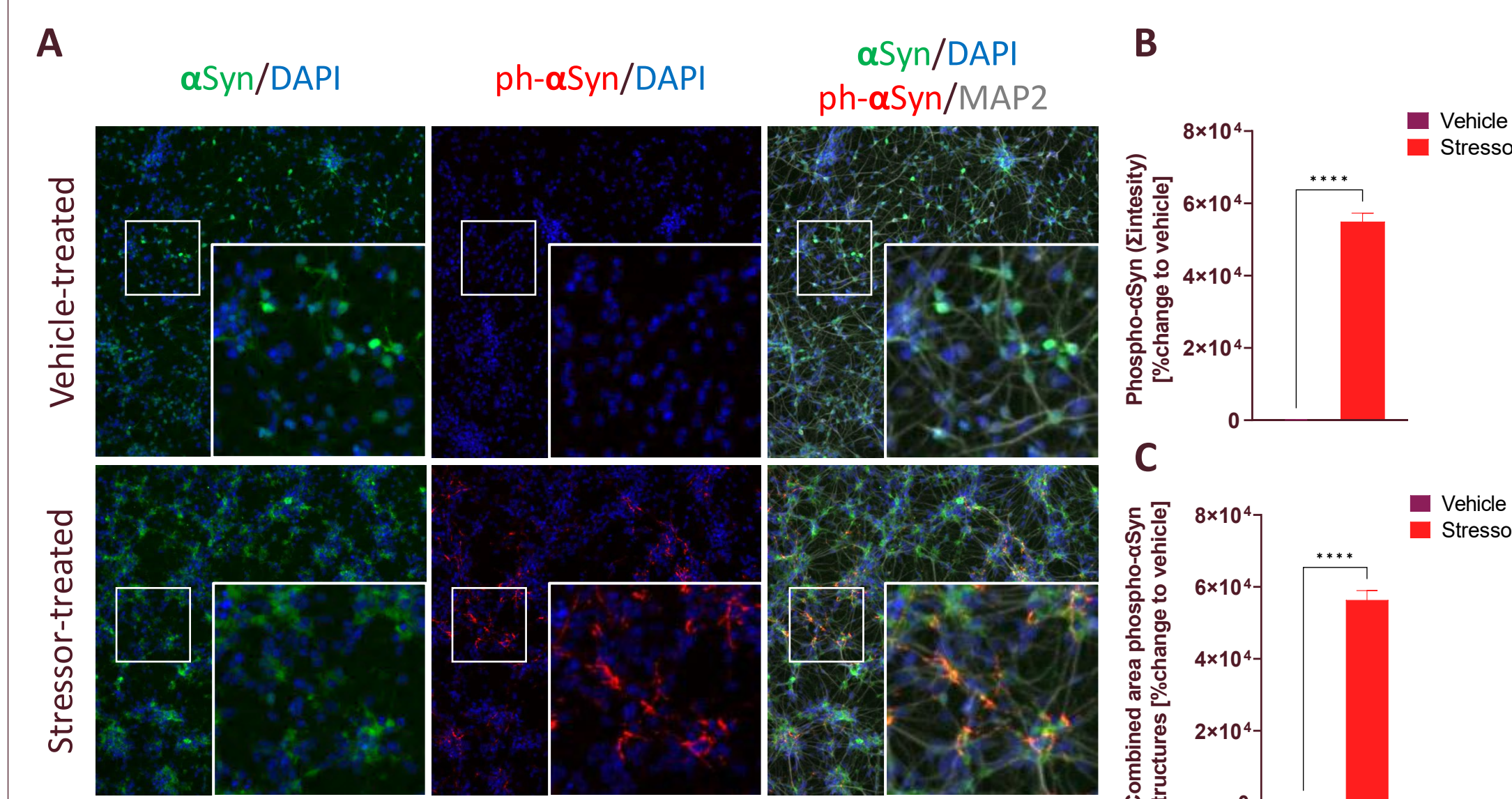


Figure 2. Staining and quantification of phospho α -Synuclein in Ncyte cortical neurons

(A) Representative ICC images of Ncyte cortical neurons vehicle-treated compared to stressor-treated. Nuclei stained with DAPI in blue, α -Synuclein in green, phospho α -Synuclein in red and MAP2 in grey. Zoom-in of relevant structures in bottom-right. (B) Quantification of p- α Syn intensity and (C) area in Ncyte cortical neurons stressor-treated normalized to vehicle-treated. Mean \pm SEM, ****p<0.00001.

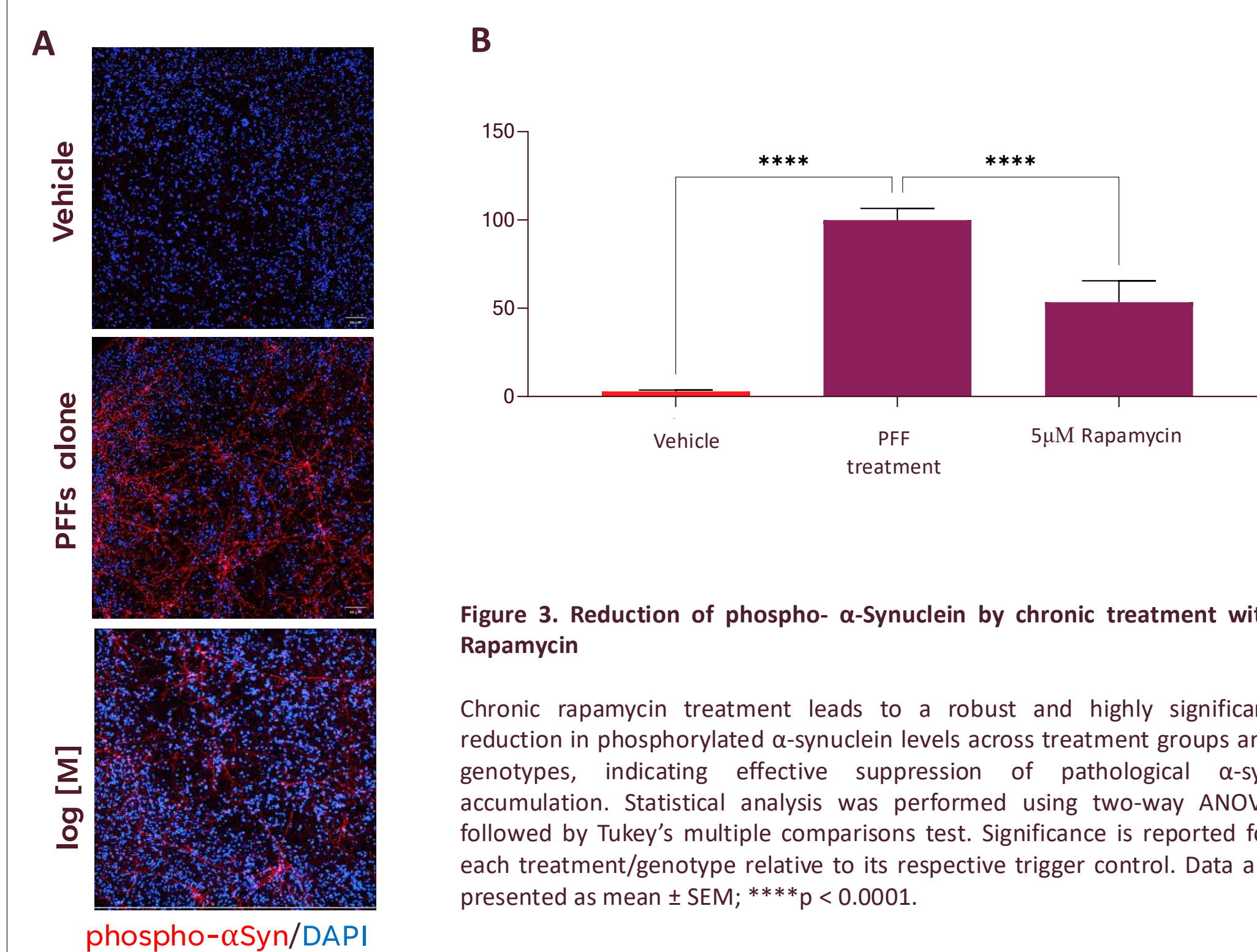


Figure 3. Reduction of phospho- α -Synuclein by chronic treatment with Rapamycin

Chronic rapamycin treatment leads to a robust and highly significant reduction in phosphorylated α -synuclein levels across treatment groups and genotypes, indicating effective suppression of pathological α -syn accumulation. Statistical analysis was performed using two-way ANOVA followed by Tukey's multiple comparisons test. Significance is reported for each treatment/genotype relative to its respective trigger control. Data are presented as mean \pm SEM; ****p < 0.0001.

TDP-43 proteinopathies

Ncardia's TDP-43 proteinopathy model in motor neurons (MNs)* demonstrates, (1) mislocalization of TDP-43 to the cytoplasm, (2) an increase in neurofilament-L (NF-L) secretion as compared to controls, (3) reduction in STMN2 protein levels and (4) electrophysiological deficits by MEA.

(1) Mislocalization of TDP-43 to the cytoplasm and pathological TDP-43 aggregate formation

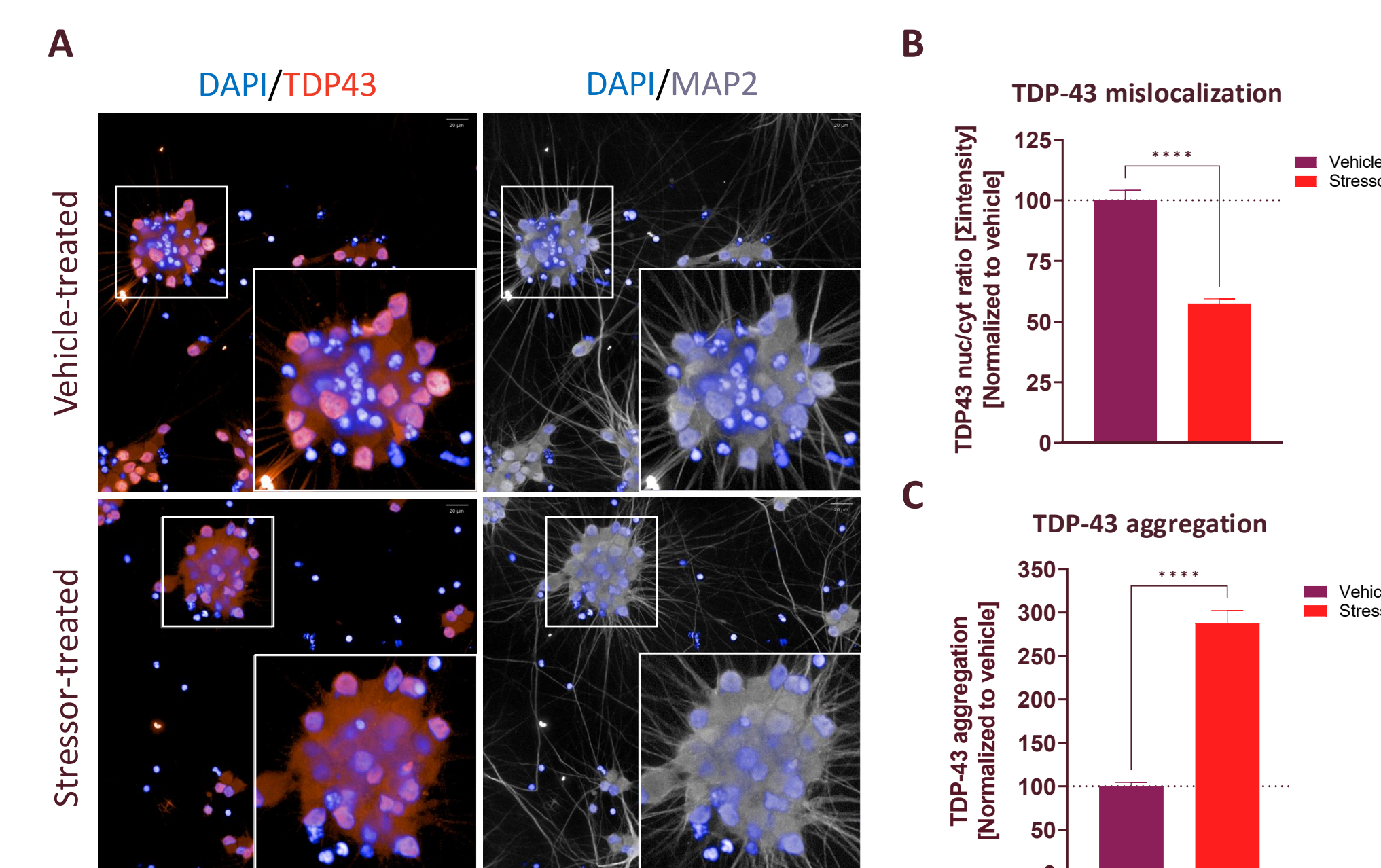


Figure 4. Mislocalization of TDP-43 to the cytoplasm and pathological TDP-43 aggregate formation

(A) HCI images (40 \times) of vehicle- vs stressor-treated TDP-43 mutant MNs. DAPI (blue), TDP-43 (red), MAP2 (grey); inset shows zoomed region.

(B) Nuclear/cytoplasmic TDP-43 intensity ratio, normalized to vehicle-treated MNs.

(C) TDP-43 aggregation in stressor-treated mutant MNs and hiPSC-derived astrocytes, normalized to vehicle. Data shown as mean \pm SEM; ****p<0.00001.

(2) Neurofilament-L release in TDP-43 mutant MNs

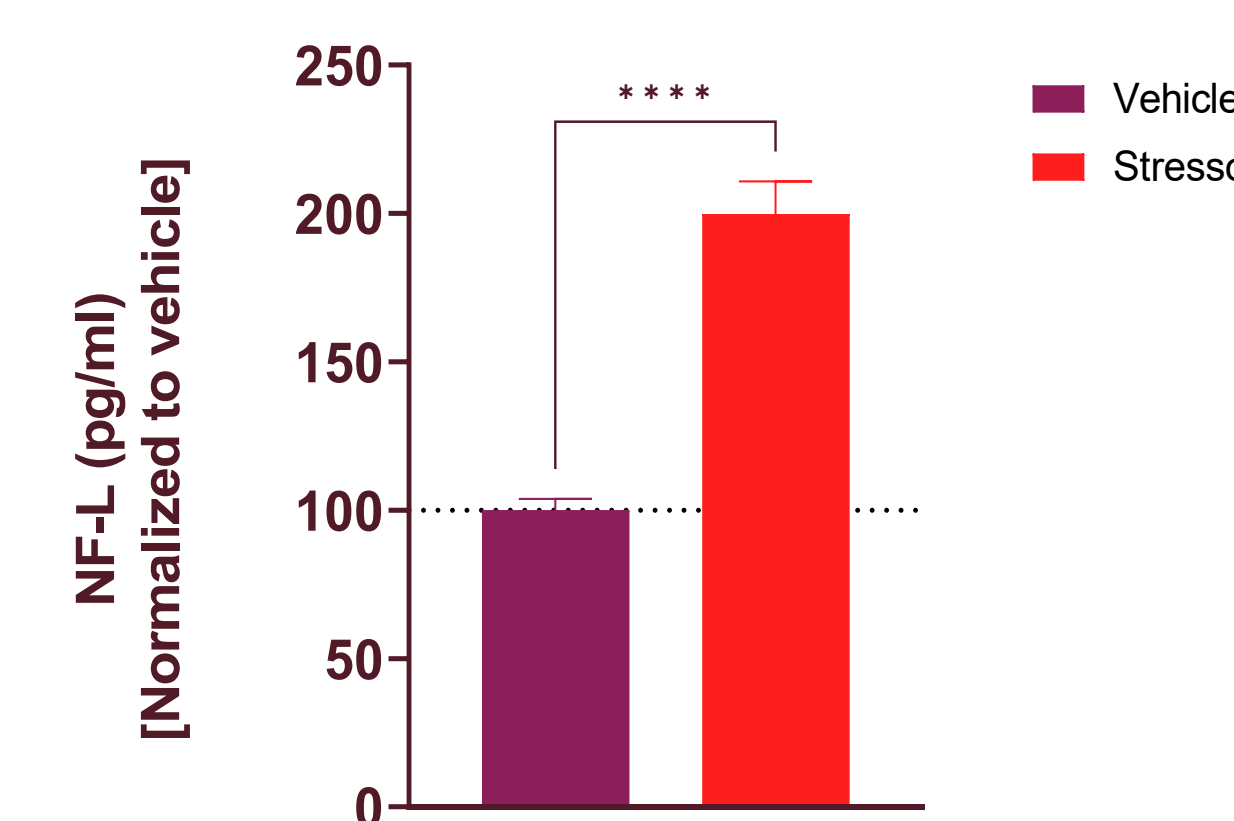


Figure 5. Quantification of neurofilament-L release of TDP-43 mutant MNs

Quantification of Neurofilament-L (NF-L) in supernatants of TDP-43 mutant MNs treated with a stressor normalized to vehicle-treated TDP-43 MNs. Error bars represent mean \pm SEM, ****p<0.00001.

(3) Quantifiable reduction of STMN2 protein and mis-splicing of STMN2 gene

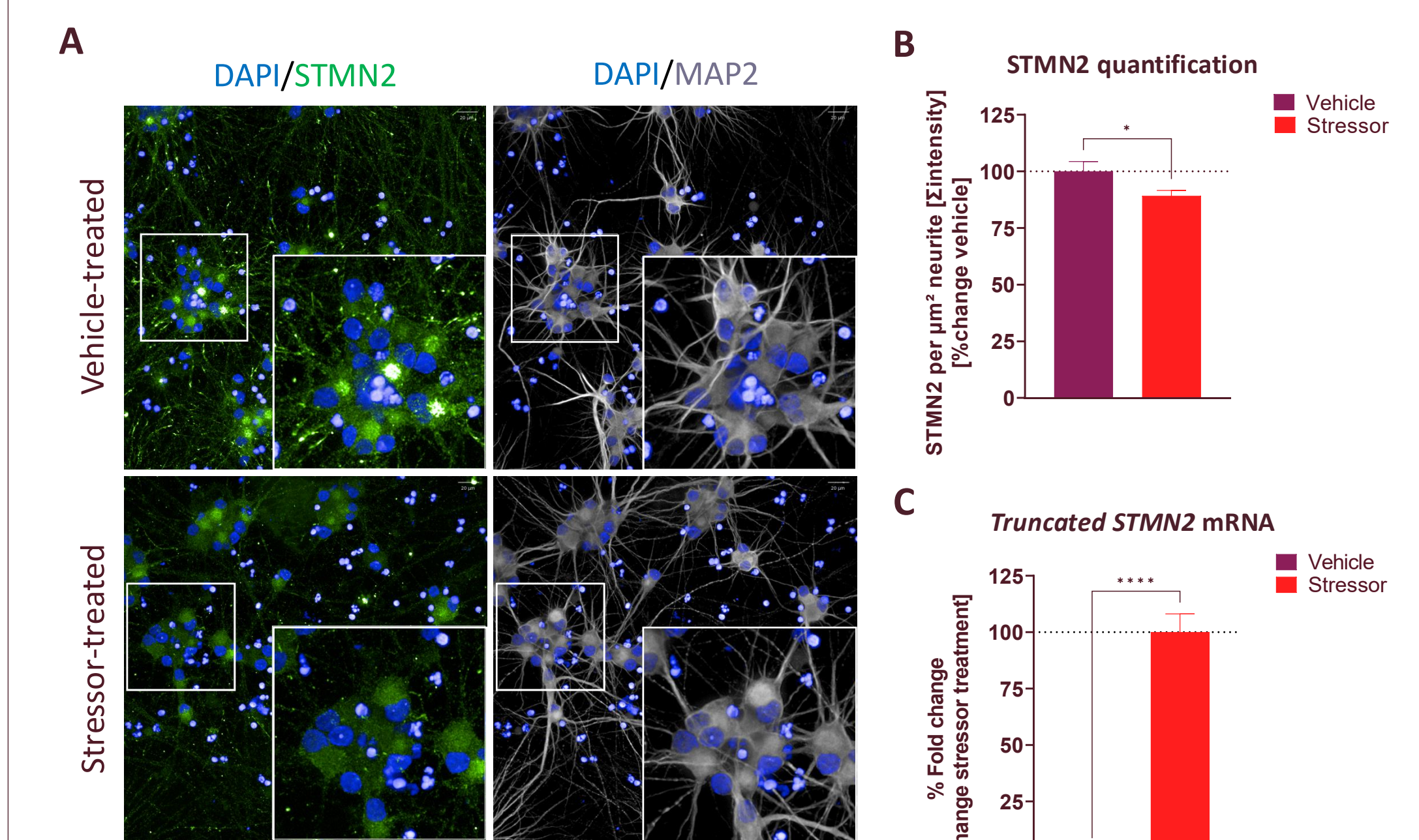


Figure 6. Reduction of STMN2 protein and mis-splicing of STMN2 gene

(A) HCI images (40 \times) of vehicle- vs stressor-treated TDP-43 mutant MNs. DAPI (blue), STMN2 (green), MAP2 (grey); inset shows zoomed region.

(B) STMN2 summed intensity per μ m² in MAP2⁺ neurites, normalized to vehicle-treated MNs.

(C) Truncated STMN2 mRNA levels in stressor-treated mutant MNs, normalized to stressor-treated controls. Data shown as mean \pm SEM; *p<0.05, ****p<0.00005.

(4) Altered electrophysiological properties of TDP-43 MNs in complex coculture with astrocytes

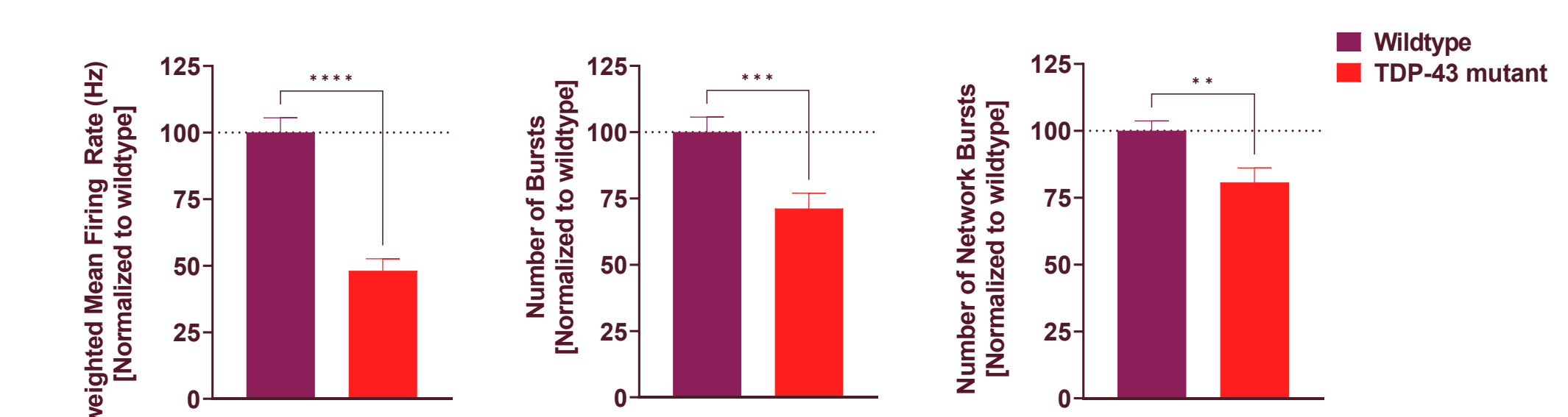


Figure 7. Electrophysiological properties of wildtype and TDP-43 mutant MNs in coculture with hiPSC-derived astrocytes**

Quantification of electrophysiological activity of wildtype and TDP-43 mutant MNs. Mean firing rate (Hz), number of bursts and network bursts. Error bars represent mean \pm SEM, **p<0.001, ***p<0.0001, ****p<0.00001

Conclusions

At Ncardia, we have developed a scalable platform, based on physiologically-relevant cellular models which can be leveraged for the high-throughput screening of drug candidates targeting the reduction of pathological propagation and accumulation of proteins in tauopathies, synucleinopathies and TDP-43 proteinopathies.

Scalable platforms for screening of drug candidates for Tauopathies, Synucleinopathies and TDP-43 proteinopathies

